Increased trends in global extreme fire weather driven predominantly by atmospheric humidity and temperature

Piyush Jain (piyush.jain@canada.ca)
Northern Forestry Centre https://orcid.org/0000-0002-0471-4663
Dante Castellanos-Acuna
University of Alberta
Sean Coogan
University of Alberta
John Abatzoglou
University of California, Merced https://orcid.org/0000-0001-7599-9750
Mike Flannigan
University of Alberta

Article

Keywords: fire weather, climate change, fire risk, wildfire

Posted Date: June 11th, 2021

DOI: https://doi.org/10.21203/rs.3.rs-595210/v1

Version of Record: A version of this preprint was published at Nature Climate Change on November 25th, 2021. See the published version at https://doi.org/10.1038/s41558-021-01224-1.

Increased trends in global extreme fire weather driven predominantly by atmospheric humidity and temperature

Piyush Jain[1,*], Dante Castellanos-Acuna[2], Sean C. P. Coogan[2], John T. Abatzoglou[3], Mike D. Flannigan[2]

[1]Natural Resources Canada, Canadian Forest Service, Northern Forestry Centre, Edmonton, AB, Canada. Email: piyush.jain@canada.ca

[2]Department of Renewable Resources, University of Alberta, Edmonton, AB, Canada. Email: scoogan@ualberta.ca; dcastell@ualberta.ca; mike.flannigan@ualberta.ca

[3]Management of Complex Systems, University of California, Merced, CA, USA. Email: jabatzoglou@ucmerced.edu

Correspondence: piyush.jain@canada.ca

Running head: Global trends in fire weather

Abstract

Climate and weather greatly influence wildfire, and recent increases in wildfire activity have been linked to climate change. However, the atmospheric drivers of observed changes have not been articulated globally. We present a global analysis of trends in extreme fire weather from 1979–2020. Significant increases in extreme (95^{th} percentile) annual values of the Fire Weather Index (FWI_{95}), Initial Spread Index (ISI_{95}), and Vapour Pressure Deficit (VPD_{95}) occurred over 26.0%, 26.1%, and 46.1% of the global burnable landmass, respectively. Significant trends corresponded to a 35.8%, 36.0%, and 21.4% increase in mean global FWI_{95}, ISI_{95}, and VPD_{95}, respectively. Relative humidity and temperature were identified as the drivers of significant trends in FWI_{95} and ISI_{95} in most regions, largely where temperature trends outpaced dew point trends. We identified relatively few regions in which wind speed or precipitation were drivers. These findings have wide-ranging implications for understanding fire risk in a changing climate.

Climate and weather greatly influence global wildland fire (Abatzoglou et al. 2018). Climate influences the type and distribution of vegetation (fuels), and weather is a main driver of regional fire activity (Littell et al. 2009; Abatzoglou and Kolden 2013). Especially important to wildland fire management are the periods of extreme fire weather that lead to fast spreading fires that resist suppression and are responsible for the majority of burned area (e.g., Hanes et al. 2019), often with catastrophic impacts (Wang et al. 2017). Recent decades have experienced an increase in the number of large and destructive wildfires in many regions (Flannigan et al. 2009a; Dennison et al. 2014; Hanes et al. 2019), and nearly all recent extreme wildfire events have occurred under extreme fire weather conditions (Bowman et al. 2017). In the future, occurrence of extreme fire weather is expected to increase in many areas due to climate change (Coogan et al. 2019; Abatzoglou et al. 2019).

Extreme fire weather is typically evaluated using fire weather indices that incorporate daily weather variables related to fuel moisture and fire behaviour. Several indices are used across the globe including the Canadian Fire Weather Index System (FWI; Van Wagner 1987). The FWI System is adaptable to different regions and is relatively easy to implement, being based on air temperature, relative humidity (RH), windspeed (WS), and precipitation (Van Wagner 1987; Wotton 2009) — these weather variables have all been shown to strongly influence the occurrence, behaviour, and effect of wildfires (Flannigan and Harrington 1988; Flannigan et al. 2016) including changes in fire season characteristics over the observational record (Jain et al. 2017; Jolly et al., 2015). While Jolly et al. (2015) noted the most significant changes in global fire weather season length were co-located in areas where changes in temperature, RH, WS, and rain-free intervals were most pronounced, they did not attribute the relative importance of individual meteorological variables on season length.

This study seeks to understand observed changes in extreme fire weather globally using modern reanalysis data (ERA5; Hersbach et al. 2020) from 1979–2020, and further elucidate the dominant meteorological variables behind the change. We use the ERA5 reanalysis to estimate and examine trends in select FWI System variables including the Initial Spread Rate (ISI) and the FWI index. The ISI combines WS and surface fuel moisture content to give an index of a fire's rate of spread and is a useful indicator across a range of forest types (Wotton 2009). The FWI index combines ISI and the build-up index (BUI; a measure of cumulative fuel dryness) and represents potential fire intensity (Amiro et al. 2004; Flannigan and Harrington 1988). We also examined trends in the vapor pressure deficit (VPD), a metric which provides a measure of the atmosphere's capacity to extract moisture from surface vegetation. High VPD values brought about by the combination of high temperatures and a dry airmass can, over an extended period, result in increased fuel flammability due to loss of moisture to the atmosphere, and several studies have found linkages between VPD and fire ignitions, growth, and burned area (Sedano and Randerson 2014; Williams et al. 2014, 2019; Mueller et al. 2020). Lastly, while fire regime changes have been linked to climate change (Abatzoglou and Williams 2016; Kirchmeier-Young et al. 2019), the variables driving such changes have not been globally articulated. For this reason, and given the nonlinear nature of the FWI System, we attribute the dominant meteorological variables (i.e., FWI System inputs) responsible for trends in ISI and FWI extremes globally.

Global trends in the 95th percentile of FWI, ISI, and VPD

70 We evaluated trends in extreme fire weather by focussing on the 95th percentile of the annual
71 values of FWI, ISI, and VPD (denoted FWI_{95}, ISI_{95}, and VPD_{95}, respectively) from 1979–2020
72 (see methods for details). We also report these trends by the global biome classification shown in
73 Fig. 1 and use only the fire season estimated for each biome-continent combination to determine
74 annual distributions from which the percentile values are derived. Significant positive trends in
75 annual FWI_{95} occurred over 26.0% of the burnable global land mass (Fig 2a; Table 1). There
76 were, however, important regional variations in the observed trends (Fig 2a; Table 1; Tables S2
77 and S3). Positive trends in FWI_{95} occurred predominantly in western North America (e.g.,
78 subtropical desert, subtropical mountain system, temperate desert, temperate mountain system
79 west), South America (e.g., tropical moist forest south, tropical rainforest), Africa (e.g.,
80 subtropical mountain system, tropical desert, tropical moist forest north, tropical rainforest),
81 western Europe (e.g., subtropical dry forest, temperate continental forest, temperate steppe), and
82 eastern Australia (e.g., subtropical dry forest), while the greatest percentage of negative trends
83 occurred in India (covered predominantly by the tropical shrubland and tropical dry forest west
84 biomes). Similar patterns were also seen for trends in annual ISI_{95} values, with significant
85 positive trends occurring over 26.1% of the global burnable land mass (Fig. 2b; Table 1). In
86 contrast to FWI_{95} and ISI_{95}, significant positive trends in annual VPD_{95} values occurred over
87 46.1% of the global burnable lands (Fig. 2c; Table 1), albeit with similar spatial variation.
88 Conversely, significant negative trends in FWI_{95}, ISI_{95}, and VPD_{95} were found for <2.5% of
89 global burnable lands.

90 Altogether, for the entire global burnable area the mean value over the 41-year period for
91 FWI_{95} increased by 13.3% (i.e. from 29.8 to 33.8), while ISI_{95} increased by 11.5% (from 12.6 to
92 14.0), and VPD_{95} increased by 12.3% (from 26.6 to 29.9). Considering only areas that

93 experienced significant trends, the mean changes were larger, corresponding to a 35.8% (i.e.
94 from 34.4 to 46.7), 36.0% (from 12.8 to 17.4), and 21.4% (from 27.9 to 33.7-hPa) increase in
95 mean global FWI_{95}, ISI_{95}, and VPD_{95}, respectively (Table 1).

96 The greatest percentage of significant trends showing increases in FWI_{95}, ISI_{95} and
97 VPD_{95} tended to occur in tropical, subtropical, and temperate biomes (see Tables S2 and S3). It
98 is important to note, however, that extreme wildfire events are generally limited by fuel
99 availability in low productivity climates and by mesic conditions in very productive climates
100 (Pausas et al. 2013; Bowman et al. 2017), with the latter exhibiting more robust links to
101 variability in FWI and VPD (e.g., Abatzoglou et al., 2018). However, productive tropical
102 ecosystems can be an exception to this in areas where people set fires for agricultural purposes
103 and to clear rainforest (Cochrane 2003). There were also increasing trends in extreme fire
104 weather in boreal ecosystems, which have experienced a relatively high proportion (26.8%) of
105 extreme wildfire events worldwide (Bowman et al. 2017), although the significance and size of
106 these trends were generally smaller compared with tropical, subtropical, and temperate biomes
107 (Tables S2, S3 and S4). While the polar biome showed relatively few significant trends in ISI_{95}
108 and FWI_{95}, there were positive trends in VPD_{95} across 37.6% of polar burnable area (Table 1).
109 Increasing extreme fire weather in the Arctic in combination with increased lightning activity
110 (Chen et al. 2021) increases the probability of extreme wildfire occurrence and impact, which
111 may have strong implications for the expansion of the boreal forest into the Arctic and for the
112 global carbon cycle through carbon release from peat fires (Turetsky et al. 2015). It should also
113 be noted that in India, which showed the greatest deceases in extreme fire weather, negative
114 trends in humidity (Fig. S2) may have been dominated by land use changes (Prijith et al. 2021).

The observed spatial patterns of positive significant trends in historical fire weather extremes shown here are consistent with earlier studies that include the European Mediterranean (Giannaros et al. 2021), North America (Jain et al. 2017), and Australia (Clarke et al. 2017). Globally, Jolly et al. (2015) found significant lengthening of the potential fire season over a quarter of the earth's vegetated surface, based on analysis of several fire weather indices between 1979 and 2013. However, the focus of that study was changes in fire season length, whereas in the present study we have examined trends in extreme fire weather during a fixed fire season. Additionally, our analysis is based on the newer ERA5 reanalysis with higher spatial resolution and extends the period of analysis from 1979 to 2020. Noting that, globally, the seven warmest years on record have occurred since 2014 (NOAA 2021), the most recent decade may have been instrumental in driving extreme fire weather trends and may indicate an emerging climate change signal.

Fire weather trends are predominantly driven by atmospheric humidity and temperature

To investigate the drivers of the observed significant trends in FWI_{95} and ISI_{95}, we conducted a partial Mann-Kendall test (pMK; see methods) where we considered the four FWI System input variables as covariates (i.e., temperature, precipitation, RH, and WS), as well as VPD. The pMK test is a method for detecting multivariate trends that can ascertain whether a covariate has an influence on the trend of a response variable. If any trend in the response variable that was originally determined to be statistically significant is no longer significant after accounting for the covariate and repeating the test, then the covariate has a significant influence on the detected trend. We refer to such covariates as *drivers* of a significant trend in the response variable. Using

this method, RH and temperature were identified as the drivers of significant trends in FWI_{95} in more grid cells (Fig. 3) and for more biomes and continents (Tables 2, S2 and S3) than WS or precipitation. Globally, RH was attributed as a driver of FWI_{95} for 75.0% of grid cells with significant trends, while temperature, precipitation, and WS each accounted for 40.4%, 11.3%, and 10.6% of significant grid cells, respectively. Results for ISI_{95} were quantitatively similar (see Fig. S2); RH was attributed as a driver of ISI_{95} for 82.2% of grid cells with significant trends, and temperature, precipitation, and WS each accounted for 40.2%, 13.4%, 11.6% of significant grid cells, respectively. Because RH was the most frequent driver of significant trends in both FWI_{95} and ISI_{95}, we also examined the covariance between these response variables and VPD (Table 2 and Table S5). Globally, VPD exhibited a significant covariance with 61.6% of grid cells that had significant trends in FWI_{95}, and a significant covariance with 59.1% of grid cells that had significant trends in ISI_{95}.

The trend attribution analysis presented here (i.e., pMK) does not explicitly consider correlations between covariates. Notably, temperature is correlated with both RH and VPD, most directly through the saturated vapor pressure (e_s), which represents the vapor pressure at which the air is in equilibrium with liquid water. RH and VPD also depend on the actual vapor pressure (e_a), which depends on the dew point temperature (Td). To investigate these relationships further we further examined trends in 2m noon temperature (T) and Td, and their influence on trends in the extreme fire weather metrics considered here (Fig. 4a,b). Significant positive trends in T were found for 73.5% of the global burnable landmass, with negative significant trends accounting for only 0.4%. In contrast, significant positive trends for Td were found for 44.3% of the global burnable landmass, with negative significant trends found in 12.4% of the same area. Overall, locations with both positive T and Td trends occurred for 68.3% of all observed trends.

160 Moreover, increasing T and decreasing Td accounted for 27.1% of all trends, decreasing T and
161 increasing Td accounted for only 3.3% of all trends, and both negative T and Td trends
162 accounted for only 1.3% of all trends. Interestingly, there were regional differences in directions
163 of observed T and Td trends; for some regions with significant positive trends in T (e.g., North
164 American and Eurasian Boreal), Td trends were also positive, whereas in other regions with
165 significant positive T trends (e.g., Western US, Amazon, Southern Africa), Td trends were
166 negative (Fig. 4a,b).

167 We also examined significant trends in FWI_{95}, ISI_{95} and VPD_{95} as a function of trends in
168 T and Td (Fig. 4c,d,e). For all three variables, positive trends co-occurred predominantly where
169 T trends outpace Td trends, a condition that occurred for 99.4%, 99.3% and 90.9% of the
170 identified positive significant trends in FWI_{95}, ISI_{95} and VPD_{95}, respectively, whereas this
171 condition occurred for 73.5% of all global burnable lands; the strongest trends in these variables
172 occurring where trends in T were positive and those in Td were negative. In other studies,
173 increasing temperatures have been linked to decreasing atmospheric vapor pressure and related
174 humidity indices. For example, increasing summertime VPD over the continental United States
175 has been associated with a combination of increasing e_s and decreasing e_a (Ficklin and Novick
176 2017), and global trends in continental temperature and humidity have both been linked to ocean
177 warming (Bryne and O'Gorman 2018).

178 Our findings are consistent with recent studies that have documented changes in the
179 weather variables that drive fire weather. For instance, Jolly et al. (2015) found a significant
180 decrease in global mean annual minimum RH, and a significant increase in global mean annual
181 maximum temperature from 1979–2013. They also found an increased trend in global mean
182 annual maximum windspeed although it should be noted that we found significant positive trends

183 in fire season mean noon wind speed were largely confined only to South America and Africa
184 (Fig. S2). Moreover, it is very likely that extreme fire weather conditions will increase into the
185 future with continued anthropogenic climate change (Flannigan et al. 2009a,b). In addition to an
186 increase in extreme fire weather, it is also likely that in the future there will be a greater number
187 of wildland fire ignitions in some regions due to climate-driven increases in lightning activity,
188 especially in the Arctic tundra and boreal forest ecosystem (Chen et al. 2021). It is therefore
189 distinctly possible that some of the regions displaying positive trends in extreme fire weather will
190 face a future with more wildland fire.

191

192 **Conclusions**

193 In conclusion, our analysis suggests that, based on three fire weather metrics, fire weather
194 extremes during the fire season have significantly increased over a quarter to nearly half of the
195 Earth's burnable surface over the past four decades (between 1979 and 2020). We demonstrate
196 that decreases in RH and increases in temperature were primarily responsible for increases in fire
197 weather extremes; conversely, changes in wind speed and daily precipitation were responsible
198 for relatively few trends globally. Further, positive trends in fire weather extremes
199 overwhelmingly occurred when trends in temperature outpace trends in dew point temperature.
200 Moreover, although approximately half to three quarters of the global burnable landmass showed
201 no significant trend in extreme fire weather over the entire time period, with continued global
202 warming and regional aridification, we may expect some of these areas to experience significant
203 future increases in extreme fire weather. Moreover, areas already exhibiting significant trends
204 should expect further increases in extreme fire weather in the future given probable climate

change scenarios (Flannigan et al. 2009a). Thus, it is likely that the world faces a future with more extreme occurrence of wildland fire in which we will have to adapt accordingly.

There are, however, a few caveats to our analysis. For one, both the ISI and FWI, like all FWI System variables, are qualitative — fuel type needs to be accounted for to generate quantitative values of fire behaviour. Furthermore, the threshold values of FWI and ISI that may demarcate extreme fire weather may not be equivalent in different ecosystems; however, by focussing on the 95th percentile of these values we show that trends in the extreme values of these variables have increased, decreased, or did not experience a trend in particular biomes and continents. Note that we also examined the 75th percentiles of FWI, ISI, and VPD and found the results to be similar, indicating our results are not overly sensitive to the choice of percentile. It should also be mentioned that the pMK test we used to determine drivers of FWI_{95} and ISI_{95} is a test that determines which variables display significant covariance with observed trends but is not equivalent to a sensitivity analysis. Thus, although trends in precipitation and WS did not covary with FWI_{95} and ISI_{95} in as many biomes as RH and temperature, they are still important inputs of the FWI system and in determining fire weather, and it should be noted that that both WS and precipitation were still identified as drivers in a few specific parts of the world. The identification of location-specific drivers of extreme fire weather may be useful for verifying the outputs of climate models that aim to predict future fire weather indices. Finally, we used defined fire seasons for our analysis, but these may be changing over time, as there have been observed increases in fire season length in several regions as well as globally.

Wildfire management is challenging at the best of times, but the increasing demands on fire management agencies operating in complicated multiple-use landscapes has made it even more difficult (Tymstra et al. 2019). Extreme fire weather drives wildland fire activity, and such fire weather, as defined by FWI_{95}, ISI_{95}, and VPD_{95}, has increased across 26–46% of the global burnable landmass. Our analysis thus supports the hypothesis that extreme fire weather has increased world wide. Furthermore, many of the regions identified as having positive trends in extreme fire weather have in recent decades experienced extreme wildfire events, some of which were disastrous, including parts of western North America, South America, Europe, southern Africa, Russia, and Australia (Bowman et al. 2017). We may see even more catastrophic fires in the future due to climate change, as we expect the increasing trend in extreme fire weather to cover more regions of the world and for fire weather to become even more extreme. Without changes in fire management practices, climate change is expected to increase the economic costs of fire suppression (Hope et al. 2016) and may lead to fire seasons that overwhelm fire suppression agencies (Podur and Wotton 2010; Abatzoglou et al. 2021). Thus, although wildfire management is adaptive, significant changes may be required in the future as the current status quo may no longer be a viable option in areas of the world facing increasing extreme fire weather.

Data Availability

The hourly ERA5 data used for this study are available from: https://doi.org/10.24381/cds.adbb2d47. The derived fire weather metrics that support the findings of this study are also available from the corresponding author upon reasonable request.

Acknowledgements

We would like to thank the Canadian Partnership for Wildland Fire Science for their support.

Author contributions

P.J. and M.F. designed the initial study. All authors contributed to discussions regarding the further development of the study design and analysis. D.C-A., P.J. and J.T.A. performed the analysis. S.C.P.C. and P.J. wrote the manuscript. All authors contributed to the review and revision of the manuscript.

Competing interests statement

The authors declare no competing interests.

References

1. Abatzoglou JT, Kolden CA (2013) Relationships between climate and macroscale area burned in the western United States. International Journal of Wildland Fire 22, 1003–1020. doi:10.1071/WF13019
2. Abatzoglou JT, Williams AP (2016) Impact of anthropogenic climate change on wildfire across western US forests. Proceedings of the National Academy of Sciences USA 113, 11770-11775.
3. Abatzoglou JT, Williams AP, Boschetti L, Zubkova M, Kolden CA (2018) Global patterns of interannual climate-fire relationships (2018) Global patterns of interannual climate-fire relationships. Global Change Biology 24, 5164-5175.
4. Abatzoglou JT, Williams AP, Barbero R (2019) Global emergence of anthropogenic climate change in fire weather indices. *Geophysical Research Letters*, 46(1):326–336.
5. Abatzoglou JT, Juang CS, Williams AP, Kolden CA, Westerling AL (2021) Increasing synchronous fire danger in forests of the western United States. Geophysical Research Letters 48, e2020GL091377.
6. Amiro BD, Logan KA, Wotton BM, Flannigan MD, Todd JB, Stocks BJ, Martell DL (2004) Fire weather index system components of large fires in the Canadian boreal forest. International Journal of Wildland Fire. 13:391-400. doi.org/10.1071/WF03066
7. Bedia J, Herrera S, Gutierrez JM, Benali A, Brands S, Mota B, Moreno JM (2015) Global patterns in the sensitivity of burned area to fire weather: implications for climate change. Agricultural and Forest Meteorology 214-215, 369-379.

8. Bowman DMJS, Williamson GJ, Abatzoglou JT, Kolden CA, Cochrane MA, Smith AMS (2017) Human exposure and sensitivity to globally extreme wildfire events. Nature Ecology and Evolution 1, 0058.
9. Bowman DMJS, Kolden CA, Abatzoglou JT, Johnston FH, van der Werf GR, Flannigan M (2020) Vegetation fires in the Anthropocene. Nature Reviews Earth & Environment 1, 500-515.
10. Cai X, Wang X, Jain P, Flannigan MD (2019) Evaluation of gridded precipitation data and interpolation methods for forest fire danger rating in Alberta, Canada. Journal of Geophysical Research: Atmospheres 124, 3-17.
11. Carvalho A, Flannigan MD, Logan K, Miranda AI, Borrego C (2008) Fire activity in Portugal and its relationship to weather and the Canadian Fire Weather Index System. International Journal of Wildland Fire 17, 328–338. doi:10.1071/WF07014
12. Chen Y, Romps DM, Seeley JT, Veraverbeke S, Riley WJ, Mekonnen ZA, Randerson JT (2021) Future increases in Arctic lightning and fire risk for permafrost carbon. Nature Climate Change. doi: 10.1038/s41558-021-01011-y
13. Clarke H, Lucas C, Smith P (2013) Changes in Australian fire weather between 1973 and 2010. International Journal of Climatology 33, 931-944.
14. Cochrane MA (2003) Fire science for rainforests. Nature 421, 913–919.
15. Coogan SCP, Robinne F-N, Jain P, Flannigan MD (2019) Scientists' warning on wildfire — a Canadian perspective. Canadian Journal of Forest Research 49, 1015-1023.
16. de Jong MC, Wooster MJ, Kitchen K, Manley C, Gazzard R, McCall FF (2016) Calibration and evaluation of the Canadian Forest Fire Weather Index (FWI) System for

improved wildland fire danger rating in the United Kingdom. Natural Hazards and Earth System Sciences 16, 1217-1237.

17. de Groot WJ, Flannigan MD, Cantin AS (2013) Climate change impacts on future boreal fire regimes. Forest Ecology and Management 294, 35-44.
18. de Groot WJ, Wotton, BM, Flannigan MD (2015) Wildland fire danger rating and early warning systems. In Hazards and Disasters Series: Wildfire Hazards, Risks and Disasters. Edited by D. Paton, P.T. Buergelt, S. McCaffrey, and F. Tedim. Elsevier, Amsterdam, Netherlands. pp. 1169 207-228.
19. Dennison PE, Brewer SC, Arnold JD, Moritz MA (2014) Large wildfire trends in the western United States, 1984-2011. Geophysical Research Letters 41, 2928-2933.
20. Dupuy J-L, Fargeon H, Martin-StPaul N, Pimont F, Ruffault J, Guijarro M, Hernando C, Madrigal J, Fernandes P (2020) Climate change impact on future wildfire danger and activity in southern Europe: a review. Annals of Forest Science 77, 35.
21. Evangeliou N, Kylling A, Eckhardt S, Myroniuk V, Stebel K, Paugam R, Zibstev S, Stohl A (2019) Open fires in Greenland summer 2017: transport, deposition and radiative effects of BC, OC and BrC emissions. Atmos. Chem. Phys. 19, 1393–1411.
22. Flannigan MD, Harrington JB (1988) A study of the relation of meteorological variables to monthly provincial area burned by wildfire in Canada (1953-80). Journal of Applied Meteorology 27, 441-452.
23. Flannigan MD, Logan KA, Amiro BD, Skinner WR, Stocks BJ (2005) Future area burned in Canada. Climatic Change 72, 1-16. doi.org/10.1007/s10584-005-5935-y

24. Flannigan MD, Krawchuck MA, de Groot WJ, Wotton BM, LM Gowman (2009a) Implications of changing climate for global wildland fire. International Journal of Wildland Fire 18, 483-507.
25. Flannigan MD, Stocks B, Turetsky M, Wotton M. 2009b. Impacts of climate change on fire activity and fire management in the circumboreal forest. Global Change Biol. 15: 549–560. doi:10.1111/j.1365-2486.2008.01660.x.
26. Flannigan MD, Wotton BM, Marshall GA, de Groot WJ, Johnston J, Jurko N, Cantin AS (2016) Fuel moisture sensitivity to temperature and precipitation: climate change implications. Climatic Change 134, 59-71.
27. Ficklin, D. L., & Novick, K. A. (2017). Historic and projected changes in vapor pressure deficit suggest a continental-scale drying of the United States atmosphere. *Journal of Geophysical Research: Atmospheres*, *122*(4), 2061-2079.
28. Forsyth GG, van Wilgen BW (2008) The recent history of the Table Mountain National Park and implications for fire management. Koedoe Afr. Prot. Area Conserv. Sci 50, 3–9.
29. Giannaros, T. M., Kotroni, V., & Lagouvardos, K. (2021). Climatology and trend analysis (1987–2016) of fire weather in the Euro-Mediterranean. International Journal of Climatology, 41, E491-E508.
30. Good P, Moriondo M, Giannakopoulos C, Bindi M (2008) The meteorological conditions associated with extreme fire risk in Italy and Greece: relevance to climate model studies. International Journal of Wildland Fire 17, 155–165. doi:10.1071/WF07001
31. Hanes CC, Wang X, Jain P, Parisien M-A, Little JM, Flannigan MD (2019) Fire-regime changes in Canada over the last half century. Canadian Journal of Forest Research 49, 256-269.

32. He T, Lamont BB, Pausas JG (2019) Fire as a key driver of Earth's biodiversity. Biological Reviews 94, 1983-2010.

33. Holz A, Paritsis J, Mundo IA, Veblen TT, Kitzberger T, Williamson GJ, Aráoz E, Bustos-Schindler C, González ME, Grau HR, Quezada JM (2017). Southern annular mode drives multicentury wildfire activity in southern South America. PNAS 114, 9552–9557.

34. Hope ES, McKenney DW, Pedlar JH, Stocks BJ, Gauthier S (2016) Wildfire suppression costs for Canada under a changing climate. PLoS ONE 11, e0157425.

35. Jain P, Wang X, Flannigan MD (2017) Trend analysis of fire season length and extreme fire weather in North America between 1979 and 2015. International Journal of Wildland Fire 26, 1009-1020.

36. Jolly WM, Cochrane MA, Freeborn PH, Holden ZA, Brown TJ, Williamson GJ, Bowman DM (2015) Climate-induced variations in global wildfire danger from 1979 to 2013. Nature Communications 6, 7537. doi:10.1038/NCOMMS8537

37. Kirchmeier-Young MC, Gillet NP, Zwiers FW, Cannon AJ, Anslow FS (2019) Attribution of the influence of human-induced climate change on an extreme fire season. Earth's Future 7, 2-10.

38. Littell JS, McKenzie D, Peterson DL, Westerling AL (2009) Climate and wildfire area burned in western US ecoprovinces, 1916-2003. Ecological Applications 19, 1003-1021.

39. Mueller SE, Thode AE, Margolis EQ, Yocum LL, Young JD, Iniguez JM (2020) Climate relationships with increasing wildfire in the southwestern US from 1984 to 2015. Forest Ecology and Management 460, 117861.

40. NOAA National Centers for Environmental Information, State of the Climate: Global Climate Report for Annual 2020, published online January 2021, retrieved on May 31, 2021 from https://www.ncdc.noaa.gov/sotc/global/202013.
41. Pausas JG, Ribeiro E (2013) The global-fire productivity relationship. Glob. Ecol. Biogeogr. 22, 728–736.
42. Prijith, S. S., Srinivasarao, K., Lima, C. B., Gharai, B., Rao, P. V. N., SeshaSai, M. V. R., & Ramana, M. V. (2021). Effects of land use/land cover alterations on regional meteorology over Northwest India. Science of The Total Environment, 765, 142678.
43. Podur J, Wotton BM (2010) Will climate change overwhelm fire management capacity? Ecological Modelling 221, 1301-1309.
44. Sedano F, Randerson JT (2014) Vapor pressure deficit controls on fire ignition and fire spread in boreal forest ecosystems. Biogeosciences 11, 1309–1353. doi:10.5194/bgd-11-1309-2014.
45. Turetsky, Merritt R., Brian Benscoter, Susan Page, Guillermo Rein, Guido R. Van Der Werf, and Adam Watts. "Global vulnerability of peatlands to fire and carbon loss." *Nature Geoscience* 8, no. 1 (2015): 11-14.
46. Tymstra C, Flannigan MD, Stocks BJ, Cai X, Morrison K (2019) Wildfire Management in Canada: Review, challenges and opportunities. Progress in Disaster Science. doi.org/10.1016/j.pdisas.2019.100045
47. van der Werf GR, Randerson JT, Giglio L, Collatz GJ, Kasibhatla PS et al. (2006) Interannual variability of global biomass burning emissions from 1997 to 2004. Atmospheric Chemistry and Physics Discussions, European Geosciences Union 6, 3175-3226.

48. Vadrevu KP, Lasko K, Giglio L, Schroeder W, Biswas S, Justice C (2019) Trends in vegetation fires in south and southeast Asian countries. Scientific Reports 9, 7422.
49. Van Wagner CE (1987). Development and structure of the Canadian Forest Fire Weather Index System. Canadian Forestry Service, Forestry Technical Report 35. (Ottawa, ON, Canada)
50. Wang, X., Thompson, D.K., Marshall, G.A., Tymstra, C., Carr, R. and Flannigan, M.D. (2015) Increasing frequency of extreme fire weather in Canada with climate change. Climatic Change. 130:573-586. doi.org/10.1007/s10584-015-1375-5.
51. Wang X, Parisien M-A, Taylor SW, Candau J-N, Stralberg D, Marshall GA, Little JM, Flannigan MD (2017) Projected changes in daily fire spread across Canada over the next century. Environmental Research Letters 12, 025005.
52. Williams PA, Seager R, Macalady AK, Berkelhammer M, Crimmins MA, Swetnam TW, Trugman AT, Buenning N, Noone D, McDowell NG, Hryniw N, Mora CI, Rahn T (2014) Correlations between components of the water balance and burned area reveal new insights for predicting forest fire area in the southwest United States. International Journal of Wildland Fire 24, 14-26. doi:10.1071/WF14023.
53. Williams AP, Abatzoglou JT, Gershunov A, Guzman-Morales J, Bishop DA, Balch JK, Lettenmaier DP (2019) Observed impacts of anthropogenic climate change on wildfire in California. Earth's Future 7, 892–910.
54. Wotton BM (2009) Interpreting and using outputs from the Canadian Forest Fire Danger Rating System in research applications. Environmental and Ecological Statistics 16, 107–131.

Methods

Data. We used the recently released ERA5 reanalysis data to provide the meteorological variables required for input into the calculation of the FWI System variables FWI and ISI (see below). The ERA5 global reanalysis is a fifth-generation product produced by the European Centre for Medium-range Weather Forecasts (ECMWF) that replaced the ERA-Interim. The large spatial coverage of reanalysis data typically offers a better alternative to weather station data for larger-scale analyses such as this, while the ERA5 reanalysis offers several improvements over earlier reanalysis products and its predecessor, the ERA-Interim (Copernicus Climate Change Service 2017; Hersbach et al. 2020). One key improvement is that ERA5 offers much higher spatial and temporal resolution by providing hourly analysis fields for 137 levels (from the surface up to a height of 80 km) on a 31-km horizontal grid. Various studies have shown ERA5 improves on other surface weather reanalyses, with respect to wind speeds (Ramon et al. 2019), precipitation (Beck et al. 2019) and for hydrological modeling (Tarek et al. 2020), for example. We downloaded ERA5 hourly single pressure level (surface) data from 1979–2020 (available from https://cds.climate.copernicus.eu/cdsapp#!/dataset/reanalysis-era5-single-levels?tab=overview).

We categorized global regions by biome based on Olsen et al. (2001). Biomes that were >1,000,000 ha were split into smaller ecoregions based on the latest classification from World Wildlife Fund (Dinerstein et al. 2017). In total, we partitioned the globe into 20 biomes (Fig. 1a); further stratification by continent resulted in 105 distinct regions (biomes × continents).

We downloaded global fire data from the Global Fire Atlas (GFA), which is based on the MODIS satellite record (Andela et al. 2019), for estimation of fire season length for each biome

(see below). The GFA provided day of burn at 500-m resolution for each year from 2003–2016. Many regions of the globe were affected by wildfires each year as indicated by the mean annual percentage of area burned by biome (Fig. 1b).

FWI calculation. We used the ERA5 reanalysis to estimate the FWI System variables ISI and FWI for our global trend analysis. Both ISI and FWI provide numeric ratings of relative wildland fire potential, and are based on tracking moisture in multiple fuel layers using surface weather variables. The calculation of these FWI System components is based on daily observations of temperature, RH, WS, and 24-hour accumulated precipitation (Van Wagner 1987).

The ERA5 meteorological data required preprocessing before calculating FWI and ISI. For temperature, we used *2m temperature* (the air temperature 2 m above the surface), where units were converted from K to °C. We calculated *2m relative humidity* from *2m temperature* and *2m dew point temperature* based on equations 1 and 2 in McElhinny et al. (2020). We calculated *10m windspeed* (WS) in km/hr from the *10m* U (zonal velocity) and V (meridional velocity) wind components, as required by the FWI System. Finally, we used *hourly total precipitation* to calculate *24 hour accumulated precipitation,* which was converted to units of mm. All variables were obtained for noon local time to provide daily inputs as required for the FWI System calculations.

Using these inputs, we calculated the ISI and FWI according to the methods outlined in McElhinny et al. (2020). Adjustments were made for regions with seasonal snow cover by using a meteorological proxy for continuous snow cover at each grid cell to determine when to stop the calculation. Specifically, maximum daily temperature (Tmax) was used to determine when the

462 FWI was to be deactivated (after 3 consecutive days with Tmax <5°C) and reactivated (after 3
463 consecutive days with Tmax >12°C) as per Wotton and Flannigan (1993). In addition, an
464 overwintering procedure was then applied to adjust the spring start-up value of the drought code
465 (DC; an FWI System component, and input into the FWI index, that provides a numeric rating of
466 the average moisture content of deep, compact organic layers) based on the amount of
467 overwinter precipitation.

468

469 **Fire season estimation.** As we are interested in fire weather trends during the fire season, we
470 estimated the observed fire season for each biome using data from the Global Fire Atlas (Andela
471 et al. 2019). We aggregated the day of burn fire data (2003 to 2016) over each biome and then
472 defined the biome-level fire season as the minimum number of months that accounted for at least
473 90% of the area burned for each biome (Table S1).

474

475 **Vapor Pressure Deficit.** VPD was calculated using the hourly ERA5 *2m temperature* and *2m*
476 *dewpoint temperature* using the conversion equation from Alduchov and Eskridge (1996) and
477 implemented in the R package 'bigleaf' (Knauer et al. 2018).

478

479 **Trend analysis.** We examined trends in the time series of ISI_{95}, FWI_{95}, and VPD_{95} values at
480 each grid cell, globally. Annual values were calculated at each grid cell and for each biome from
481 1979 to 2020 (42 years in total). In each case, the annual percentile values only included data
482 contained in the observed fire season months. We further masked out barren areas using land

483 cover MODIS satellite data (Friedl et al. 2010), and defined according to the International
484 Geosphere-Biosphere Program land cover classification system (Loveland & Belward, 1997), as
485 these areas did not contain significant burnable biomass and many of these areas would
486 otherwise skew the results due to their highly arid climates (e.g., North Africa). Trend analysis
487 was performed on the time series using the Mann-Kendall (MK) test, a robust nonparametric test
488 for trend detection (Mann 1945; Kendall 1975). Linear trends were determined using the Thiel-
489 Sen estimator (Theil 1950; Sen 1968). Multiple testing and spatial autocorrelation were
490 respectively accounted for by controlling the False Discovery Rate (FDR; Wilks 2006) and by
491 setting the global significance level (α_{global}) equal to 0.5 α_{FDR} (Wilks 2016). Here we set α_{global} to
492 0.05. We display the results of our significant trends in Fig. 2, 3 and 4 at this significance level.
493 The 95th percentiles we examined represent extreme values in the fire weather metrics; however,
494 we also examined trends in 50th and 75th percentiles and found similar results (results not
495 shown).

496

497 **Drivers of trends in FWI95 and ISI95.** We used the pMK test to assess the influence of
498 covariates on the trend of our response variables (Libiseller and Grimvall 2002). The pMK test
499 modifies the MK test by removing the contribution of a covariate of interest that correlates with
500 the response variable. If any trend in the response variable that was originally determined to be
501 statistically significant is no longer significant (here, tested at the α=0.05 level) after accounting
502 for the covariate and repeating the test, then the covariate has a significant influence on the
503 detected trend; in this case, we refer to the corresponding covariate as a *driver* of a significant
504 trend in the response variable. For example, Mediero et al. (2014) used this method to link trends

505 in flood metrics to increases in evapotranspiration. Here, because the four FWI inputs
506 (temperature, RH, WS, and precipitation) can combine nonlinearly to generate FWI outputs, the
507 association between the FWI_{95} or ISI_{95} and the upper (or lower) annual quantiles of the inputs
508 may not be strong. In order to determine the influence of each of the inputs, we extracted the
509 input values that corresponded to the response variable (e.g., FWI_{95} or ISI_{95}) of interest; this was
510 achieved by binning all the input values corresponding to values of the response variable in a
511 range centered on the 95th percentile (from 92.5% to 97.5%) and taking the median value of each
512 of the binned inputs.

513 The MK and pMK tests were performed using the R packages 'EnvStats' (Millard 2013)
514 and 'trend' (Pohlert 2020). The FDR correction was applied using the 'p.adjust' function in the R
515 base 'stats' package. All analyses were performed using R version 4.

516

517 **Methods References:**

518 1. Alduchov, O. A. & Eskridge, R. E., 1996: Improved Magnus form approximation of
519 saturation vapor pressure. Journal of Applied Meteorology, 35, 601-609
520 2. Andela, N., Morton, D. C., Giglio, L., Paugam, R., Chen, Y., Hantson, S., van der Werf,
521 G. R., and Randerson, J. T.: The Global Fire Atlas of individual fire size, duration, speed
522 and direction, Earth Syst. Sci. Data, 11, 529–552, https://doi.org/10.5194/essd-11-529-
523 2019, 2019.
524 3. Beck, Hylke E., Ming Pan, Tirthankar Roy, Graham P. Weedon, Florian Pappenberger,
525 Albert IJM Van Dijk, George J. Huffman, Robert F. Adler, and Eric F. Wood. "Daily

evaluation of 26 precipitation datasets using Stage-IV gauge-radar data for the CONUS." *Hydrology and Earth System Sciences* 23, no. 1 (2019): 207-224.

4. Copernicus Climate Change Service (2017) ERA5: Fifth generation of ECMWF atmospheric reanalyses of the global climate. Copernicus Climate Change Service Data Store. Available from: https://confluence.ecmwf.int/display/CKB/ERA5%3A+data+documentation Accessed: 04 March 2020.
5. Dinerstein, Eric, David Olson, Anup Joshi, Carly Vynne, Neil D. Burgess, Eric Wikramanayake, Nathan Hahn et al. "An ecoregion-based approach to protecting half the terrestrial realm." BioScience 67, no. 6 (2017): 534-545.
6. Friedl, M. A., Sulla_Menashe, D., Tan, B., Schneider, A., Ramankutty, N., Sibley, A., & Huang, X. (2010). MODIS Collection 5 global land cover: Algorithm refinements and characterization of new datasets. Remote Sensing of Environment, 114(1): 168–182
7. Knauer, J., El-Madany, T. S., Zaehle, S., & Migliavacca, M. (2018). Bigleaf—An R package for the calculation of physical and physiological ecosystem properties from eddy covariance data. *PloS one*, *13*(8), e0201114.
8. Libiseller, C., & Grimvall, A. (2002). Performance of partial Mann–Kendall tests for trend detection in the presence of covariates. Environmetrics: The official journal of the International Environmetrics Society, 13(1), 71-84.
9. Mediero, L., Santillán, D., Garrote, L., & Granados, A. (2014). Detection and attribution of trends in magnitude, frequency and timing of floods in Spain. Journal of Hydrology, 517, 1072-1088.

10. Hersbach, Hans, Bill Bell, Paul Berrisford, Shoji Hirahara, András Horányi, Joaquín Muñoz-Sabater, Julien Nicolas et al. "The ERA5 global reanalysis." Quarterly Journal of the Royal Meteorological Society 146, no. 730 (2020): 1999-2049.
11. Kendall, M. G.: 1975, Rank Correlation Methods, Griffin, London.
12. Loveland, T. R., & Belward, A. S. (1997). The IGBP-DIS global 1 km land cover data set, DISCover: First results. International Journal of Remote Sensing, 18, 3291−3295.
13. Mann, H. B.: 1945, 'Nonparametric tests against trend', Econometrica 13, 245–259.
14. McElhinny, M., Beckers, J. F., Hanes, C., Flannigan, M., and Jain, P.: A high-resolution reanalysis of global fire weather from 1979 to 2018 – overwintering the Drought Code, Earth Syst. Sci. Data, 12, 1823–1833, https://doi.org/10.5194/essd-12-1823-2020, 2020.
15. Millard SP (2013). _EnvStats: An R Package for Environmental Statistics. Springer, New York. ISBN 978-1-4614-8455-4, URL: https://www.springer.com.
16. Olson, D.M.; Dinerstein, E.; Wikramanayake, E.D.; Burgess, N.D.; Powell, G.V.N.; Underwood, E.C.; D'Amico, J.A.; Itoua, I.; Strand, H.E.; Morrison, J.C.; et al. Terrestrial Ecoregions of the World: A New Map of Life on Earth. *Bioscience* **2001**, *51*, 933–938.
17. Ramon, J., Lledo, L., Torralba, V., Soret, A., & Doblas-Reyes, F. J. (2019). What global reanalysis best represents near-surface winds?. *Quarterly Journal of the Royal Meteorological Society*, *145*(724), 3236-3251.
18. Sen, Pranab Kumar (1968), "Estimates of the regression coefficient based on Kendall's tau", Journal of the American Statistical Association, 63 (324): 1379–1389, doi:10.2307/2285891, JSTOR 2285891, MR 0258201

19. Tarek, M., Brissette, F. P., & Arsenault, R. (2020). Evaluation of the ERA5 reanalysis as a potential reference dataset for hydrological modelling over North America. *Hydrology and Earth System Sciences*, *24*(5), 2527-2544.
20. Theil, H. (1950), "A rank-invariant method of linear and polynomial regression analysis. I, II, III", Nederl. Akad. Wetensch., Proc., 53: 386–392, 521–525, 1397–1412, MR 0036489.
21. Thorsten Pohlert (2020). trend: Non-Parametric Trend Tests and Change-Point Detection. R package version 1.1.4. https://CRAN.R-project.org/package=trend
22. Wilks, D. S. (2006). On "field significance" and the false discovery rate. Journal of applied meteorology and climatology, 45(9), 1181-1189.
23. Wilks, D. (2016). "The stippling shows statistically significant grid points": How research results are routinely overstated and overinterpreted, and what to do about it. Bulletin of the American Meteorological Society, 97(12), 2263-2273.
24. Wotton, B. M., & Flannigan, M. D. (1993). Length of the fire season in a changing climate. The Forestry Chronicle, 69(2), 187-192.

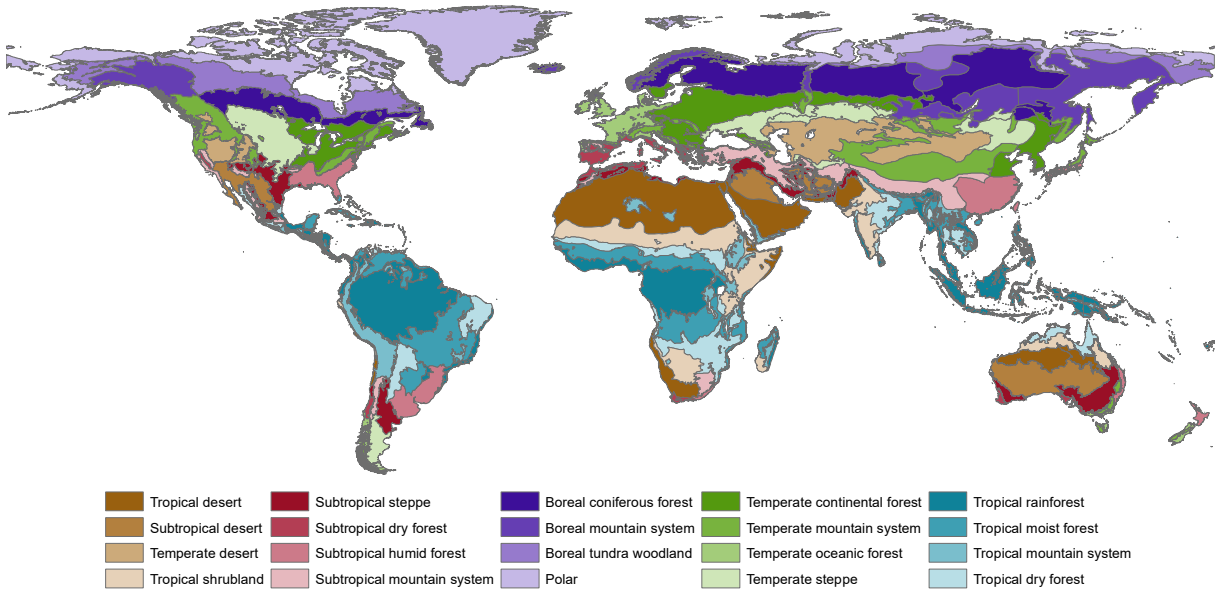

a) Map of global biomes

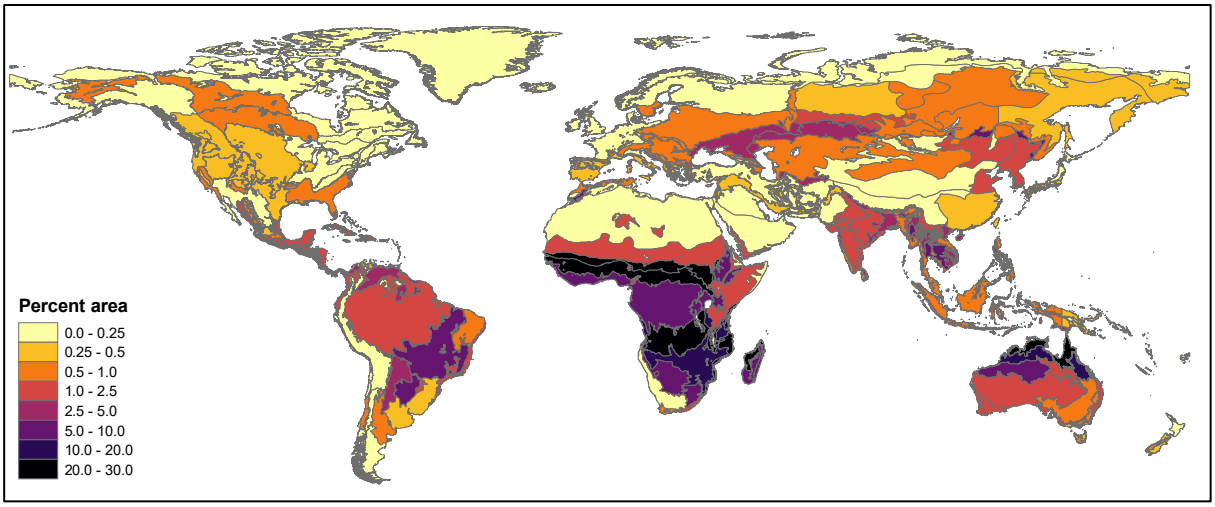

b) Mean percent annual area burned by biome

586

587 Figure 1: Global biomes modified from Olsen et al. (2001) (panel a) and corresponding annual percentage area
588 burned for the period 2003–2016 as determined from the Global Fire Atlas (Andela et al. 2019) (panel b).

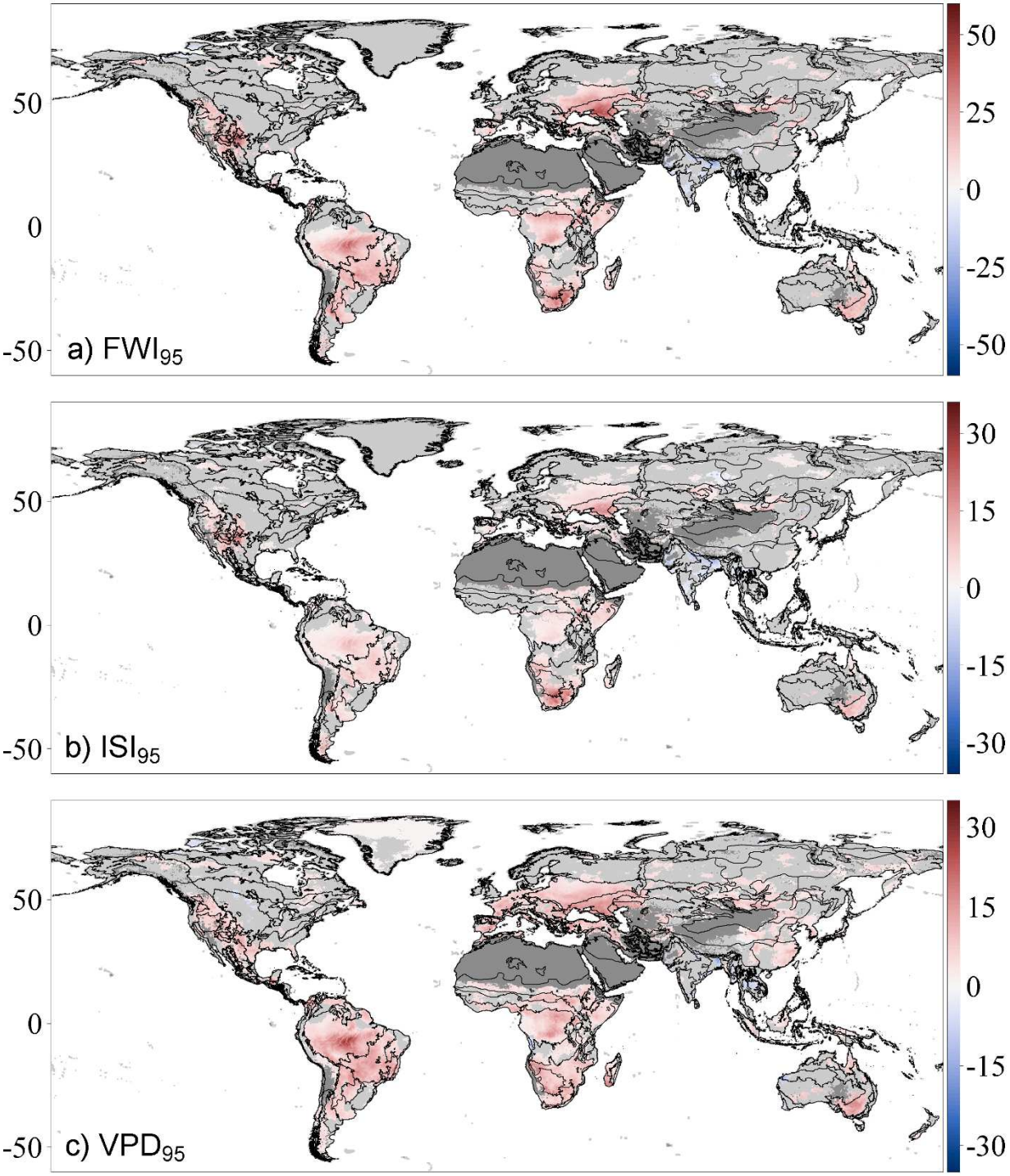

Figure 2: Significant trends (per 41y) in the annual 95th percentile of the Fire Weather Index (FWI_{95}) (Panel a), Initial Spread Index (ISI_{95}) (Panel b), and Vapour Pressure Deficit (VPD_{95}) (Panel c). Significance was determined by the Mann-Kendall trend test, controlling the false discovery rate multiple testing and adjusting for spatial autocorrelation (α=0.05). Light grey shading indicates areas where no significant trends exist, whereas areas shaded dark grey are predominantly barren (i.e., without appreciable burnable biomass) and are excluded from the calculation. Displayed trends are given by the Thiel-Sen slope estimator. Also see Fig. 1 in supplemental material for equivalent calculation showing all trends (i.e., significant and insignificant).

597

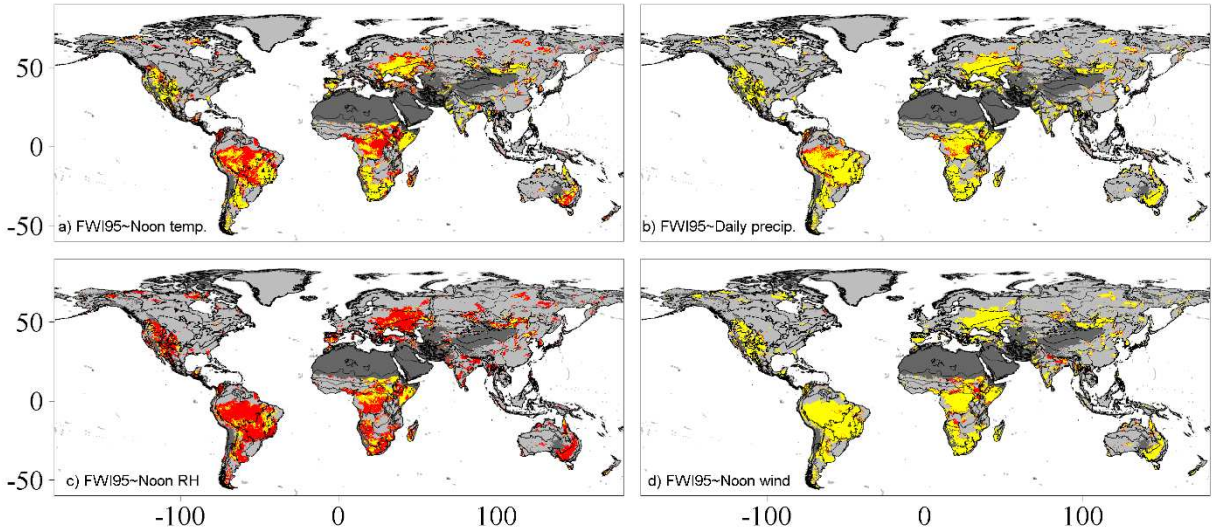

598

599 Figure 3. FWI inputs attributed as drivers of the 95th percentile of annual FWI values (FWI_{95}) as determined by the
600 partial Mann-Kendall test. Red regions indicate where significant FWI_{95} trends are no longer significant after
601 accounting for the corresponding FWI System input covariate (a. noon temperature; b. daily precipitation; c. noon
602 relative humidity (RH); and d. noon wind), thereby indicating that the covariate is a 'driver' of the observed trend.
603 Yellow regions indicate where significant trends in FWI_{95} remain significant after accounting for the covariate,
604 indicating that the corresponding FWI System input variable is not a driver of the observed trend.

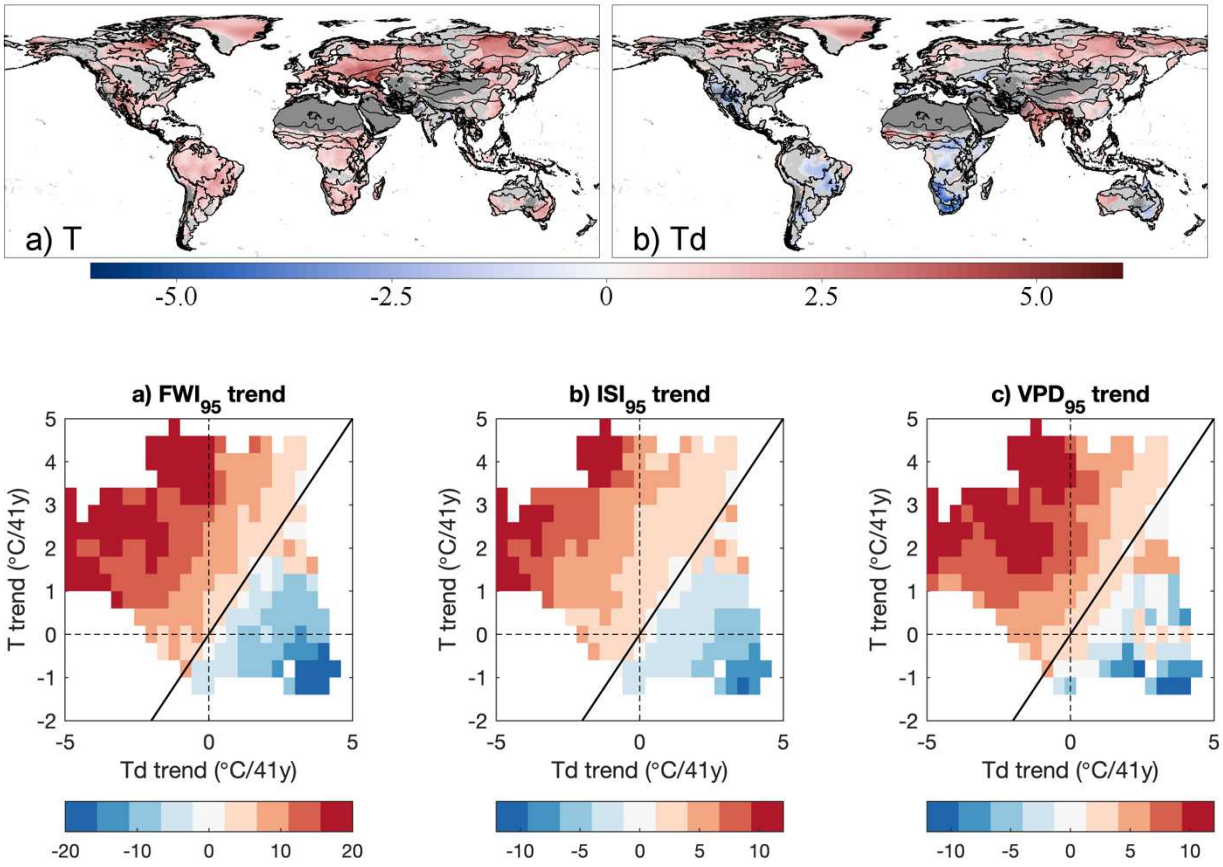

Figure 4: Significant trends (per 41y) in mean 2m temperature (T; panel a) and 2m dew point temperature (Td; panel b) during the fire season, from 1979–2020. Significant trends in FWI_{95} (panel c), ISI_{95} (panel b), and VPD_{95} (panel e) are binned to show their dependence on trends in mean fire season T and Td. Diagonal black line indicates where trends in T equal trends in Td.

Table 1: The percentage of trends that are significant for all trends (i.e., positive and negative), positive trends only, and negative trends only, for the three extreme fire weather variables (i.e., FWI_{95}, ISI_{95}, and VPD_{95}), summarised globally and by continent. Mean trend sizes (per 41yr) for all grid cells are also given, where values in parentheses are the corresponding mean trend sizes for significant trends only.

	FWI_{95}			**ISI_{95}**			**VPD_{95}**		
Percent significant	**all**	**positive**	**negative**	**all**	**positive**	**negative**	**all**	**positive**	**negative**
Global	27.8	26.0	1.8	28.6	26.1	2.5	47.7	46.1	1.5
By Continent									
Africa	55.1	53.9	1.2	52.1	50.7	1.5	77.0	75.9	1.1
Asia	22.0	15.1	6.9	23.5	13.7	9.8	47.2	43.7	3.5
Europe	18.2	17.5	0.8	22.4	20.9	1.6	34.0	33.5	0.5
North America	13.3	12.5	0.8	13.7	12.9	0.8	38.9	37.2	1.7
Oceania	23.6	23.0	0.6	20.3	19.6	0.8	28.9	26.5	2.5
South America	62.6	62.5	0.1	62.0	61.9	0.1	76.4	76.1	0.3
Mean trend size	**all (/41yr)**	**positive (/41yr)**	**negative (/41yr)**	**all (/41yr)**	**positive (/41yr)**	**negative (/41yr)**	**all (hPa/41yr)**	**positive (hPa/41yr)**	**negative (hPa/41yr)**
Global	3.9 (11.0)	6.3 (12.3)	-2.0 (-8.4)	1.4 (3.9)	2.5 (4.6)	-2.0 (-3.6)	3.2 (5.6)	4.1 (6.0)	-1.7 (-5.2)
By Continent									
Africa	7.1 (11.3)	8.1 (11.6)	-1.9 (-5.6)	3.1 (5.1)	3.7 (5.3)	-1.0 (-2.0)	5.2 (6.3)	5.6 (6.4)	-1.9 (-5.1)
Asia	1.2 (3.7)	5.0 (10.2)	-4.0 (-10)	0.2 (0.3)	2 (3.8)	-1.9 (-4.4)	2.4 (4.6)	3.9 (5.5)	-2.4 (-6.4)
Europe	3.5 (12.2)	5.0 (13.0)	-1.6 (-4.7)	1.1 (3.5)	1.8 (4.0)	-0.7 (-2.0)	3.1 (6.1)	3.6 (6.3)	-1.1 (-1.6)
North America	2.3 (11.6)	5.1 (13.1)	-1.3 (-6.7)	1.0 (4.7)	2 .0 (5.3)	-0.5 (-2.7)	1.7 (3.1)	2.3 (3.4)	-1.7 (-4.4)
Oceania	4.7 (11.7)	6.3 (12.2)	-1.8 (-5.6)	2.1 (6.1)	3.3 (6.4)	-1.4 (-3.0)	2.3 (6.5)	4.5 (7.8)	-2.2 (-6.9)
South America	8.9 (12.9)	9.7 (12.9)	-1.3 (-4.4)	3.0 (4.2)	3.3 (4.3)	-0.6 (-1.5)	6.6 (8.2)	7.0 (8.3)	-1.1 (-2.2)

Table 2: Percentage of significant trends for FWI_{95} and ISI_{95} attributable to trends in the FWI input variables temperature (T), precipitation (P), relative humidity (RH), and wind speed (WS), as well as VPD, summarised globally, by continent, and by biome. Results were determined using the partial Mann-Kendall test (see methods).

	FWI_{95}					**ISI_{95}**				
	T	**P**	**RH**	**WS**	**VPD**	**T**	**P**	**RH**	**WS**	**VPD**
Global	40.4	11.3	75.0	10.6	61.6	40.2	13.4	82.2	11.6	59.1
By continent										
Africa	40.8	9.2	58.0	15.3	59.1	43.6	13.7	67.1	16.3	58.7
Asia	34.8	14.3	79.3	18.8	59.6	29.3	12.7	85.8	19.3	52.7
Europe	38.4	11.5	84.2	6.3	55.1	32.7	13.0	90.1	8.3	50.8
North America	31.5	7.5	81.8	9.0	49.8	36.1	9.3	87.4	10.2	52.4
Oceania	43.8	7.5	89.4	12.4	69.1	39.9	7.3	92.7	10.1	62.9
South America	48.2	14.3	77.7	5.0	73.9	51.4	17.1	83.7	6.4	73.1
By biome										
Boreal coniferous forest	76.4	23.8	89.2	8.1	70.4	47.1	20.2	87.2	12.3	53.9
Boreal mountain system	45.7	18.0	74.4	12.1	59.0	35.2	17.2	89.2	16.6	45.5
Boreal tundra woodland	52.8	14.5	91.3	16.1	75.6	51.5	11.9	92.4	11.0	66.2
Polar	55.6	18.8	88.5	7.0	79.7	63.9	24.2	91.4	11.6	79.8
Subtropical desert	21.2	6.6	78.6	13.5	35.6	24.5	7.6	80.6	9.8	36.1
Subtropical dry forest	30.2	3.2	79.2	10.1	58.4	29.6	4.4	80.8	6.5	58.0
Subtropical humid forest	24.8	10.9	90.3	10.5	62.8	28.0	7.9	85.9	8.3	57.4
Subtropical mountain system	34.5	5.3	82.4	11.5	55.7	27.8	5.8	79.5	10.4	47.4
Subtropical steppe	36.3	4.5	84.1	7.2	53.9	32.5	4.5	90.8	8.8	50.5
Temperate continental forest	31.2	9.5	86.0	4.7	57.4	19.7	10.5	91.5	4.5	49.8
Temperate desert	31.9	6.4	81.1	6.0	54.5	40.3	8.2	90.7	5.6	60.3
Temperate mountain system	35.0	12.5	75.4	8.3	63.4	36.7	14.8	90.4	12.4	61.7
Temperate oceanic forest	48.5	6.2	79.6	5.0	81.5	55.8	19.2	90.0	11.7	87.5
Temperate steppe	22.2	9.2	78.4	7.5	39.9	26.3	6.7	88.4	7.5	41.3
Tropical desert	10.4	1.4	57.6	7.7	19.6	11.4	1.3	66.0	8.5	19.2
Tropical dry forest	39.8	9.1	65.8	19.4	59.5	45.0	12.0	73.1	21.4	59.1
Tropical moist forest	45.5	5.1	71.8	14.3	68.3	46.7	6.8	77.6	14.5	63.2
Tropical mountain system	57.7	25.1	68.0	15.9	68.9	53.3	24.6	70.6	14.6	64.6
Tropical rainforest	61.1	22.0	79.1	5.1	87.8	66.4	30.2	93.5	8.5	92.2
Tropical shrubland	18.8	3.6	50.4	18.9	38.8	17.9	3.7	52.4	17.5	35.1

Supplementary Files

This is a list of supplementary files associated with this preprint. Click to download.

- Globaltrendsinfireweather19792020Supplemental20200604tosubmit.pdf